Symmetric Convolutional and Adversarial Neural Network Enables Improved Mental Stress Classification From EEG

Ruiqi Fu, Yi-Feng Chen, *Member, IEEE*, Yongqi Huang, Shuping Chen, Feiyan Duan, Jiewei Li, Jianhui Wu, Dongmei Jiang, Junling Gao, Jason Gu, *Senior Member, IEEE*, Mingming Zhang, *Senior Member, IEEE*, and Chunqi Chang, *Member, IEEE*

***Abstract*—Electroencephalography (EEG) is widely used for mental stress classification, but effective feature extraction and transfer across subjects remain challenging due to its variability. In this paper, a novel deep neural network combining convolutional neural network (CNN) and adversarial theory, named symmetric deep convolutional adversarial network (SDCAN), is proposed for stress classification based on EEG. The adversarial inference is introduced to automatically capture invariant and discriminative features from raw EEG, which aims to improve the classification accuracy and generalization ability across subjects. Experiments were conducted with 22 human subjects, where each participant's stress was induced by the Trier Social Stress Test paradigm while EEG was collected. Stress states were then calibrated into four or five stages according to the changing trend of salivary cortisol concentration. The results show that the proposed network achieves improved accuracies of 87.62% and 81.45% on the classification of four and five stages, respectively, compared to conventional CNN methods. Euclidean space data alignment approach (EA) was applied and the improved generalization ability of EA-SDCAN across subjects was also validated via the leave-one-subject-out-cross-validation, with the accuracies of four and five stages being 60.52% and 48.17%, respectively. These findings indicate that the proposed SDCAN network is more feasible and effective for classifying the stages of mental stress based on EEG compared with other conventional methods.**

***Index Terms*—Adversarial learning, convolutional neural network (CNN), deep learning, electroencephalography (EEG), mental stress.**

Manuscript received December 15, 2021; revised April 20, 2022; accepted May 3, 2022. Date of publication May 18, 2022; date of current version May 31, 2022. This work was supported in part by the National Natural Science Foundation of China under Grant 61971289, in part by the Guangdong Research Program under Grant 2019ZT08Y191 and Grant 2020ZDZX3001, in part by the Natural Science Foundation of Shenzhen under Grant JCYJ20210324104203010, in part by the Shenzhen-Hong Kong Institute of Brain Science-Shenzhen Fundamental Research Institutions under Grant 2019SHIBS0003, in part by Shenzhen University (SZU) Top Ranking Project under Grant 86000000210, and in part by the Shenzhen Key Laboratory of Smart Healthcare Engineering under Grant ZDSYS20200811144003009. *(Corresponding authors: Chunqi Chang; Mingming Zhang.)*

This work involved human subjects or animals in its research. Approval of all ethical and experimental procedures and protocols was granted by the Ethics Committee of Shenzhen University under Application No. 2019049.

Ruiqi Fu is with the Health Science Center, School of Biomedical Engineering, Shenzhen University, Shenzhen 518060, China, and also with the Shenzhen Key Laboratory of Smart Healthcare Engineering, Southern University of Science and Technology, Shenzhen 518055, China (e-mail: furq@mail.sustech.edu.cn).

Yi-Feng Chen and Mingming Zhang are with the Shenzhen Key Laboratory of Smart Healthcare Engineering, Department of Biomedical Engineering, Southern University of Science and Technology, Shenzhen 518055, China (e-mail: chenyf6@sustech.edu.cn; zhangmm@sustech.edu.cn).

Yongqi Huang is with China Resources Digital Holdings Ltd., Shenzhen 518049, China (e-mail: yqi7758@163.com).

Shuping Chen and Jiewei Li are with the Health Science Center, School of Biomedical Engineering, Shenzhen University, Shenzhen 518060, China (e-mail: 13871270489@163.com; jwli@szu.edu.cn).

Feiyan Duan is with Deepbay Innovation Technology Corporation Ltd., Shenzhen 518057, China, and also with the Health Science Center, School of Biomedical Engineering, Shenzhen University, Shenzhen 518060, China (e-mail: 2150010503@szu.edu.cn).

Jianhui Wu is with the Shenzhen Key Laboratory of Affective and Social Cognitive Science, Shenzhen University, Shenzhen 518060, China (e-mail: wujh8@szu.edu.cn).

Dongmei Jiang is with the School of Computer Science, Northwestern Polytechnical University, Xi'an 710072, China, and also with the Peng Cheng Laboratory, Shenzhen 518055, China (e-mail: jiangdm@nwpu.edu.cn).

Junling Gao is with the Buddhism and Science Research Laboratory, Centre of Buddhist Studies, The University of Hong Kong, Hong Kong (e-mail: galeng@hku.hk).

Jason Gu is with the Department of Electrical and Computer Engineering, Dalhousie University, Halifax, NS B3H 4R2, Canada (e-mail: jason.gu@dal.ca).

Chunqi Chang is with the Health Science Center, School of Biomedical Engineering, Shenzhen University, Shenzhen 518060, China, and also with the Peng Cheng Laboratory, Shenzhen 518055, China (e-mail: cqchang@szu.edu.cn).

Digital Object Identifier 10.1109/TNSRE.2022.3174821

I. Introduction

MENTAL stress is defined as "the body's non-specific response to any need including emotional, cognitive, or social tasks for change" [1]. Inappropriate dealing with excessive mental stress can cause serious problems in an individual's life, which makes a reliable and accurate stress assessment technique significantly important [2]. Mental stress is generally divided into chronic stress and acute stress, the former is difficult to be modeled in either laboratory setups or clinical practices, and hence the latter is most often addressed in existing studies [3], [4]. Traditional methods to evaluate acute stress used questionnaires or stress-related hormones (e.g., cortisol) [5]–[7]. However, questionnaires are subjective and inaccurate as compared with cortisol [8]–[10]. Cortisol concentration has long been used as the first index to indicate the individual's response to stress [11], it is commonly measured through repeated blood sampling or less invasive methods such as saliva sampling [12].

In recent years, a large number of studies have shown that except for cortisol, non-invasive physiological signals such as electrodermal activity, heart rate variability, and electroencephalogram (EEG) are also affected by severe stress. Since EEG directly depicts the instant cortical response to stress [13], it has been favored by many researchers and becomes one of the most commonly used neuroimaging modalities to study stress-related brain functions [14]. Compact lightweight devices such as MindWave Mobile Headset [15] and Muse [16] are used in studies related to detecting mental stress. Various features of EEG have been employed for mental stress classification. Hjorth *et al.* [17] used frequency band power, peak frequency in the alpha band, and Hjorth parameters of EEG for stress classification. The ratio of power spectral densities (PSD) of alpha and beta bands is also used for the analysis of mental stress [18]. In [19], the PSD, correlation, differential asymmetry, and rational asymmetry are extracted from different frequency bands for two-class and three-class stress classification.

However, most existing stress classification methods calibrate the stress states by questionnaires instead of an objective biomarker such as cortisol concentration [20]–[24]. Betti et. al. [25] have shown that the features extracted from physiological signals are consistent with the trend of salivary cortisol levels. In addition, existing mental stress classification algorithms using traditional machine learning methods which highly depend on feature extraction and selection, and need to be identified by a domain expert. While deep learning neural networks can learn high-level features from data, and thus solve the problem end to end [26].

In real-life applications, we need to recognize stress as fast and conveniently as possible, which leads to end-to-end EEG-based stress classification. In [27], [28], end-to-end mental stress assessment methods based on the convolutional neural network (CNN) are presented. In [29], a 1D convolutional long short-term memory neural network (LSTM) is proposed for end-to-end stress identification using EEG. Even though CNN has been proved as an effective tool for end-to-end mental stress classification, it performs degradedly when generalizing models across subjects. The distributions of EEG data highly vary among individuals, so it is essential to explore neural activity in EEG which is invariant among individuals but discriminative to specific tasks to improve generalizability. Adversarial learning, such as generative adversarial network (GAN) [30], is designed to learn non-redundant representation from data in an unsupervised or supervised way. Adversarial theory is adopted by Ozdenizci *et al.* [31] to learn subject-invariant representations in EEG, resulting in better generalizability among subjects compared with CNN. In [32], subject-independent emotion classification based on EEG is achieved by introducing adversarial learning. Stober *et al.* [33] also proposes a convolutional autoencoder to learn transferable features across subjects.

In this paper, we propose a novel cross-subject accurate and efficient EEG-based end-to-end multi-level mental stress classification CNN integrated with adversarial inference of subject-invariant EEG features, named symmetric deep convolutional adversarial network (SDCAN), while cortisol concentration is adopted to calibrate stress stages. The major contributions of this study are summarized as follows:

(1) Instead of using questionnaires to estimate the stress levels of subjects, an accurate and objective biomarker (i.e., saliva cortisol concentration) is measured to calibrate the real stress stages.

(2) A novel end-to-end algorithm for stress classification from EEG based on deep learning is proposed, and experimental results show that the accuracy of stress classification is improved compared with state-of-the-art deep learning methods.

(3) An architecture combining CNN and adversarial theory is proposed to learn invariant and discriminative features for improved generalization ability across subjects. Experimental results demonstrated superior generalization performance of the proposed SDCAN compared with existing deep learning algorithms.

TABLE I
EXCLUSION CRITERIA VIA PRE-TELEPHONE-INTERVIEW

Exclusion criteria via pre-telephone-interview
Family history of psychiatric illnesses, neurological diseases, endocrine disorders, or major physiological illness
History of brain damage (e.g., brain surgery, cerebral hemorrhage) or severe head trauma
History use of antipsychotic drugs or cortisone
Pregnancy
Any major operation in the last 6 months
Currently in illnesses
Taking medicines or suffering from some chronic disease attacks
Smoking abuse (more than five cigarettes a day) or alcohol abuse (more than two alcoholic drinks a day)
Female subjects were tested undergoing the phase of their menstrual cycle
Female subjects who were taking birth control pills

II. MATERIALS AND METHODS

A. Participants and Apparatus

The experiment includes twenty-two participants (11 males and 11 females, aged 23.05 ± 2.25 years). All participants are recruited through online advertising and telephone interviews. In the telephone interview, each participant is informed of the experimental procedures, and all participants enrolled in this experiment are ensured not meeting any exclusion criteria as described in Table I. The experiment is approved by the Ethics Committee of Shenzhen University (2019049). All subjects have signed the informed consent forms before the experiment. In addition, to obtain salivary cortisol, participants are required to avoid drinking or eating and vigorous exercising within two hours before coming to the laboratory.

The wireless LiveAmp 32 (Brain Product GmbH, Munich, Germany) is used to record EEG during the whole period of the experiment. Saliva samples are collected using Salivettes equipment (Sarstedt, Rommelsdorf, Germany) and frozen at −40 °C until analysis. During analysis, the saliva samples are

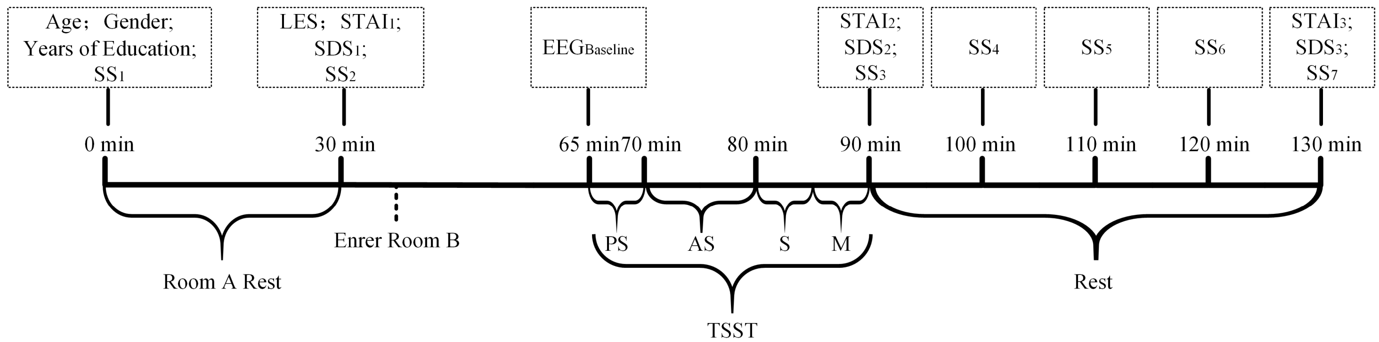

Fig. 1. The procedure of the experiment. The timeline shows the whole data-collection procedure, including demographic data, saliva sampling (SS), life event scale (LES), state trait anxiety inventory (STAI), self-rating depression scale (SDS) and EEG. PS = pre-stress period, AS = anticipatory stress period, S = speech period, M = math period.

thawed at room temperature and centrifuged at 3000 rpm for 10 minutes, then the supernatant is used to calculate the concentration of cortisol in saliva by electrochemiluminescence immunoassay (Cobas e 602, Roche Diagnostics, Numbrecht, Germany). The detection range of cortisol values by this method is 1.5-1750 nmol/L.

B. Experimental Protocol

The paradigm of this work is designed based on a modified trier social stress test (TSST) [34] as depicted in Fig. 1. The experimental setting includes two separate quiet and temperature-controlled rooms: room A as the resting place and room B as the stress-induced laboratory. The moment when the subject arrives at room A is denoted as 0 min. The subject is first asked to have a rest in room A for 30 minutes and complete questionnaires including demographic information (age, gender, years of education), life event scale (LES) [35], state trait anxiety inventory ($STAI_1$) [36], and self-rating depression scale (SDS_1) [37] at 30 min. And the first and second saliva samples (SS_1, SS_2) are also taken at 0 min and 30 min, respectively, for baseline measurements. Then the subject is guided to room B and prepared for EEG collection. Stress induction is then started at 65 min by a 25-minute TSST procedure. TSST is incorporated by a 5-minute pre-stress period, a 10-minute anticipatory stress period, a 5-minute speech period, and a 5-minute mental arithmetic period. After TSST, the subject is asked to take a 40-minute rest. Saliva samples SS_3-SS_7 are collected at 90 min, 100 min, 110 min, 120 min, and 130 min, respectively. State trait anxiety inventory and self-rating depression scale are filled at 90 min ($STAI_2$ and SDS_2) and 130 min ($STAI_3$ and SDS_3).

The EEG collection starts from the 5-minute pre-stress period and lasts throughout the next 10-minute anticipatory stress period, 5-minute speech period, 5-minute mental arithmetic period, and 40-minute rest period. In the anticipatory stress period, subjects are asked to prepare a 5-minute speech in which they should defend themselves against an assumed theft accusation, and they complete the speech in front of a video camera and three experimenters (two men and one woman), who appear in the whole TSST but not seen by the subjects before the speech session and maintain neutral facial expressions through the whole procedure, two of them wearing white coats and one wearing suit. In the mental arithmetic task, the subjects are asked to make a continuous subtraction from 1022 to 13 as quickly and accurately as possible, and they must start again from 1022 in case of error. During the 40-minute rest period, five salivary cortisol samples are collected to track the changing trend of cortisol concentration caused by TSST.

C. Data Acquisition and Pre-Processing

The 32-channel EEG data are collected continuously at a sampling rate of 500 Hz from the 65th minute of the experiment. The electrodes are located at Fp1, Fz, F3, F7, FT9, FC5, FC1, C3, T7, TP9, CP5, CP1, Pz, P3, P7, O1, O2, P4, P8, TP10, CP6, CP2, Cz, C4, T8, FT10, FC6, FC2, F4, F8, Fp2, IO according to the international 10-20 system. AFz served as the ground and FCz as the online reference. Impedance is kept below 10 k Ω for all channels.

Event markers are added to the EEG data for each subtask during the experiment. IO channel which captures the eye movements and accelerometer channels were excluded. EEG signals are bandpass filtered from 0.5 to 40 Hz by a zero-phase finite impulse response filter. The online reference was then reintroduced into the dataset, then the data were re-referenced by a common average reference. Both eye-blink and muscle artifacts are detected by visual inspection and manually removed after independent component analysis. To perform the analysis, EEG data are selected from 65th to 110th minute including all TSST stages and part of recovery. A 2-second time window with no overlap is used for EEG data slicing. EEG acquisition and preprocessing are described in the first two parts of Fig. 2, with EEG preprocessing performed using EEGLAB [38]. Among the 22 subjects in this study, the EEG data of 21 subjects are used (the data of subject 1 cannot be used due to equipment error).

D. Network Structure

The overall system architecture for evaluating the stress states from EEG signals is shown in Fig. 2. The network structure proposed in this work combines CNN with adversarial theory by adopting the architecture of GAN.

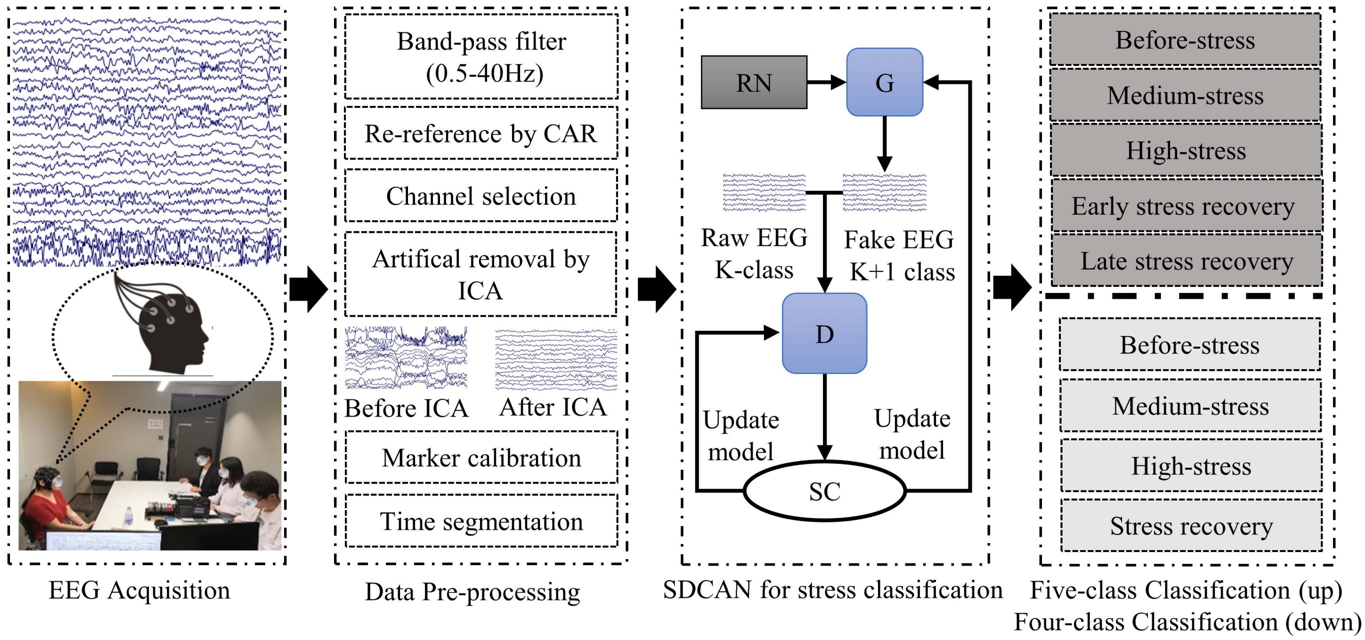

Fig. 2. An overview of stress classification framework, RN = random noise, G = generative network, D = discriminative network, SC = stress classification.

In this section, by modifying the generator and discriminator of semi-supervised learning GAN (SSL-GAN) proposed by [39], a network structure named SDCAN is proposed, in which the generator and discriminator are also two symmetrical CNNs. Unlike SSL-GAN which is designed for image classification, SDCAN achieves end-to-end EEG time series decoding. The details of the proposed network are shown in Fig. 3, in which the discriminator and generator both consist of 5 layers of convolutional or deconvolutional layers. The generator takes random noise as input and outputs the generated EEG which has the same data format as the real EEG, while the discriminator takes the multi-class real EEG data as well as the generated data as input and outputs the probability distribution that the data comes from the generated data or the one class of the multi-class real data.

The multi-class real EEG signals are denoted as $\{(x_i, y_i)_{i=1}^{K}\}$, where K represents the number of classes, $x_i \in \mathbf{R}^{C \times T}$ represents an EEG data with C channels and T sampling points, and $\{y_i \in 1 \ldots K\}$ is the corresponding class label. The discriminator includes 4 convolution-max-pooling blocks, with the convolution network in the first block split into a temporal convolutional layer and a spatial convolutional layer. Exponential linear units (ELUs) is used as the activation function in each block, and the amount of convolution kernels is gradually added from 25 in the first block to 200 in the fourth block, while the stride is set as 1 for all blocks. The generator consists of 5 layers of deconvolution with the number of kernels gradually decreasing from 200 to 1, almost symmetrical to the discriminator. The stride of each kernel is set as 2 in the first 4 layers and 1 in the last layer, and the rectified linear unit (ReLU) is used as the activation function after each deconvolution layer. In the last layer of the discriminator, the traditional GAN uses the sigmoid function to give the probability distribution of whether the data comes from the original data set or the generated data set, which makes the discriminator of the traditional GAN be regarded as a binary classifier, and the loss function of the traditional GAN is given by (1) [29].

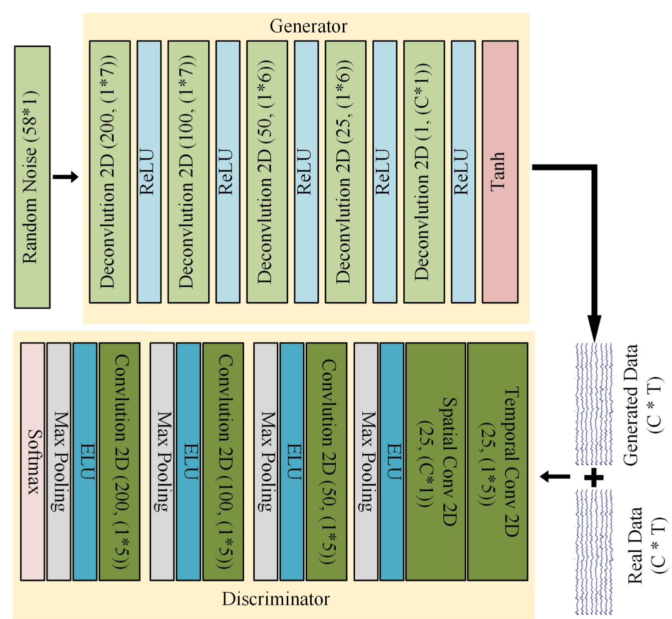

Fig. 3. The details of the proposed SDCAN model. C represents the number of channels of input data, and T represents the number of time points of input data.

$$\min_{G}\max_{D} V(D, G) = E_{x \sim p_{data(x)}}[\log D(x)] + E_{z \sim p_{z(z)}}[\log(1 - D(G(z)))] \quad (1)$$

where $p_z(z)$ represents the distribution of noise variables, $G(z)$ represents mapping noise variables into real data space, $p_{data}(x)$ represents the distribution of real data x, $D(x)$ represents the probability that x came from the real data rather than generated data, and $V(D, G)$ represents the two min-max games played by the generator and discriminator.

In this paper, the last layer of the discriminator is modified to make a multi-class classifier. Given the K-class dataset $\{(x_i, y_i)_{i=1}^{K}\}$, where $x \sim p(x|y)$, $y \sim p(y)$, the last layer of the discriminator classifies the data point x into one of the K classes with the k-dimensional logic vector $\{l_1, \ldots, l_K\}$ by applying the softmax function (2).

$$p_{\bmod el}\left(y = j \mid x\right) = \frac{\exp\left(l_j\right)}{\sum_{k=1}^{K} \exp\left(l_k\right)} \tag{2}$$

In the training process of the discriminator, the generated data is marked as $y = K + 1$, so the output dimension of the discriminator was $K + 1$ instead of K. Assuming that half of the dataset were real data and the other half were generated data (but in fact, the percentage of real data and generated data is arbitrary), by maximizing the expectation $E_{x,y\sim p}\left[\log p_D\left(y \mid x, y \leq K\right)\right]$ and minimizing the expectation $E_{x\sim p_G}\left[\log p_D\left(y = K + 1 \mid x\right)\right]$ at the same time, the loss function of the SDCAN is shown in (3).

$$\min_G \max_D E_{x,y\sim p}\left[\log p_D\left(y \mid x, y \leq K\right)\right] + E_{x\sim p_G}\left[\log p_D\left(y = K + 1 \mid x\right)\right] \tag{3}$$

where p is the distribution of real data, p_G is the distribution of generated data, p_D is the probability distribution of the discriminator, K represents the number of classes, and $K + 1$ represents the label of generated data, G represents mapping noise variables into real data space, D represents the probability that x came from the real data rather than generated data, $p_D\left(y = K + 1 \mid x\right)$ represents the probability distribution from the generated data correspond with $1 - D(G(z))$ in (1), $\log p_D(y \in 1, \ldots K|x)$ represents the probability distribution of real data which needs to be maximized. The algorithm is given in Algorithm 1.

Algorithm 1

Input: training set $\{(x_n, y_n)\}_{n=1}^{K}$, random noise $\{z^{(1)}, \ldots, z^{(m)}\}$.
Output: generated data $\left(x_{K+1}, y_{K+1}\right)$, probability distribution from D.
Initialize: Initialize model parameters: θ_d, θ_g.
While θ_d, θ_g has not converged **do**
  for iteration <= 5 **do**
    Sample $\{z^{(i)}\}_{i=1}^{m} \sim p_z(z)$ from noise prior samples;
    Sample $\{x_n^{(i)}\}_{n=1}^{K} \sim p_{\text{data}}$ from the real data;
    Update the discriminator by ascending its stochastic gradient:
    $\nabla_{\theta_d} \frac{1}{m} \sum_{i=1}^{m} \left[\log p_D\left(y \mid x, y \leq K\right) + \log p_D(y = K + 1|x)\right]$;
  end for
  Sample $\{z^{(i)}\}_{i=1}^{m} \sim p_z(z)$ from noise prior samples;
  Update the generator by descending its stochastic gradient:
  $\nabla_{\theta_g} \frac{1}{m} \sum_{i=1}^{m} \left[\log\left(1 - D\left(G\left(z^{(m)}\right)\right)\right)\right]$;
end while

n represents the label of each data pair, K represents the number of label categories, z represents the input random noise.

E. Evaluation and Statistics

Accuracy, precision, recall, and f1-score for classification evaluation are calculated based on the four parameters: true positive (*TP*), false positive (*FP*), true negative (*TN*), and false negative (*FN*), as follows:

$$\text{Accuracy} = \frac{TP + TN}{TP + FP + FN + TN} \tag{4}$$

$$\text{Precision}_i = \frac{TP_i}{TP_i + FP_i} \tag{5}$$

$$\text{Recall}_i = \frac{TP_i}{TP_i + FN_i} \tag{6}$$

$$\text{F1-Score}_i = \frac{2^* Precision_i^* Recall_i}{Precision_i + Recall_i} \tag{7}$$

where i represents the ith class regarded as a positive class, and the rest are unified as negative classes. However, considering the unbalanced samples of classes, the weighted precision, recall, and f1-score are calculated as follows:

$$\text{Precision}_{\text{weighted}} = \frac{\sum_{i=1}^{N} Precision_i{}^* w_i}{|N|} \tag{8}$$

$$\text{Recall}_{\text{weighted}} = \frac{\sum_{i=1}^{N} Recall_i{}^* w_i}{|N|} \tag{9}$$

$$\text{F1-Score}_{\text{weighted}} = \frac{2^* Precision_{weighted}{}^* Recall_{weighted}}{Precision_{weighted} + Recall_{weighted}} \tag{10}$$

where N is the total samples in all classes, i represents the ith class regarded as a positive class, and w_i is the ratio of the sample size of ith class to the total sample size.

F. Training Strategy

For classification, all EEG data are randomly divided into training, validation, and test sets by 8:1:1. The network is trained and tested by 10-fold cross-validation. Furthermore, leave-one-(subject)-out-cross-validation (LOOCV) is adopted for inter-individual cross-subject stress classification. The EEG data are divided into a training set of 20 subjects and a test set of one subject to implement LOOCV. The process is repeated 21 times to ensure that the EEG data of each subject is used as a test set. All the models are trained on an NVIDIA Tesla K80 GPU, with CUDA 10.0 using the Tensorflow API.

G. Statistical Analysis

Statistical analyses are performed to evaluate questionnaires, cortisol concentrations, and classification performance. One-way repeated-measures analysis of variance (ANOVA) is used for testing statistically significant differences between multiple groups. The paired student's t-tests are used to determine the statistical significance of the difference between different statistics. Normality and variance homogeneity are assured before applying ANOVA.

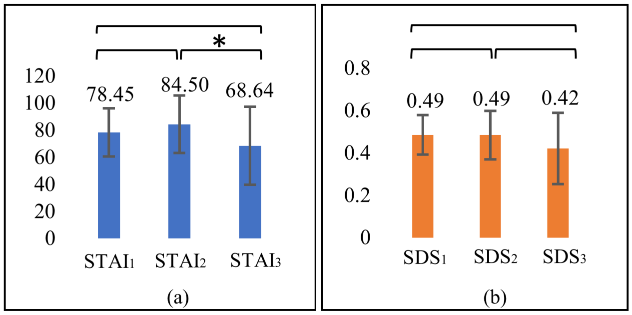

Fig. 4. Statistical results of state trait anxiety inventory (STAI) (a) and self-rating depression scale (SDS) (b) according to questionnaires at pre-TSST($STAI_1$ and SDS_1), the end of TSST($STAI_2$ and SDS_2) and during recovery($STAI_3$ and SDS_3) after TSST, respectively. The asterisk (*) indicates the significante difference with $p < 0.05$.

III. Results

A. Questionnaires and Salivary Cortisol Data Analysis

The statistical results of STAI (i.e., $STAI_1$, $STAI_2$, and $STAI_3$) and SDS (i.e., SDS_1, SDS_2, and SDS_3) according to questionnaires at pre-TSST, the end of TSST and during recovery after TSST, respectively, are shown in Fig. 4. The results do not reflect significant changes in the stress state of the subjects before and after stress induction except for STAI ($p < 0.05$), which indicates the inaccuracy of the questionnaire due to its subjectiveness. Furthermore, LES score is 21.14 ± 13.14, which shows no stressful events happened in their life recently.

The statistical results of salivary cortisol concentration values of all subjects before and after the TSST are shown in Fig. 5 (a). Considering the 20-minute time lag between hormone response and stress stimulation [4], the changing trend of salivary cortisol concentration values matched what was described in [25] that cortisol concentration value will gradually ascend due to the stimulation of TSST and gradually descend after TSST. To be concrete, SS_2 shows no significant difference compared with SS_1, and the values of SS_1 and SS_2 are relatively low, indicating subjects maintained relaxation during the rest period before 30 min; SS_3 ascends significantly compared with SS_2, indicating that the start of the anticipatory stress period of TSST at 70 min causes the change in stress state; SS_4 ascends significantly compared with SS_3, indicating that the commencement of speech period at 80 min causes changes in stress state again; SS_5 shows no significant difference compared with SS_4 and the values of SS_4 and SS_5 are relatively high, indicating that there are no stress state changes during the speech and math periods and subjects are under stress from 80 min to 90 min; SS_6 descends significantly compared with SS_5 indicating that subjects start to recover from stressful states as the end of TSST at 90 min.

Hormonal responses generally begin 20 minutes after stress stimulation, while physiological responses are almost in real-time [4]. Considering the 20-minute time lag between hormone response and physiological response, and the changing trend of the salivary cortisol concentration values also provide an objective contribution for establishing the stress response in subjects, the stress response can be divided into 4 different stages, as shown in Fig. 5 (b).

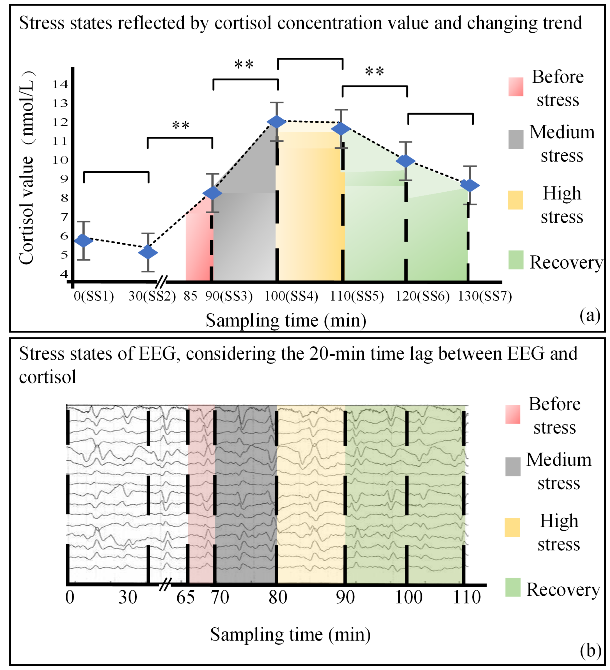

Fig. 5. Statistical results of cortisol concentration values (saliva sampling, SS) (a). The asterisk indicates significant difference, * indicates $p < 0.05$, ** indicates $p < 0.01$. Stress states of EEG (b).

B. Data Labeling

The four stages of stress indicated by changing trend of cortisol values during the experiment and the corresponding segmentation of EEG shown in Fig.5 (b) can be described as: (1) state before stress (65th -70th minute), (2) state of medium stress (70th - 80th minute), (3) state of high stress (80th - 90th minute) and (4) state of stress recovery (90th - 110th minute). Considering that stress recovery takes a long time and the corresponding salivary cortisol value decreases from 90 min to 110 min, the last state can be divided into (4) state of early stress recovery (90th - 100th minute) and (5) state of late stress recovery (100th - 110th minute). Therefore, we have either four classes or five classes of stress states in this study.

C. Benchmarking and Parameter Optimization

1) Benchmarking: To illustrate the performance of the proposed SDCAN model, we conducted extensive experiments using the state-of-the-art EEG decoding deep learning models including EEGNet [40], Deep ConvNet, and Shallow ConvNet [41], the existing CNN models with adversarial theory [31], and also traditional classifiers linear discriminant analysis (LDA) and support vector machine (SVM) [19].

Since the performance of deep learning models varies from different parameters, we performed parameter optimization among the EEGNet, Deep ConvNet, and Shallow ConvNet models for obtaining the optimal models, those models were trained with a fixed learning rate (lr) of 0.001 but various batchsize. The batchsize leading to the best classification performance in each of the corresponding models (four-class/five-class Deep/Shallow ConvNet and EEGNet) is used for further comparison. As shown in Fig. 6, after 10-fold

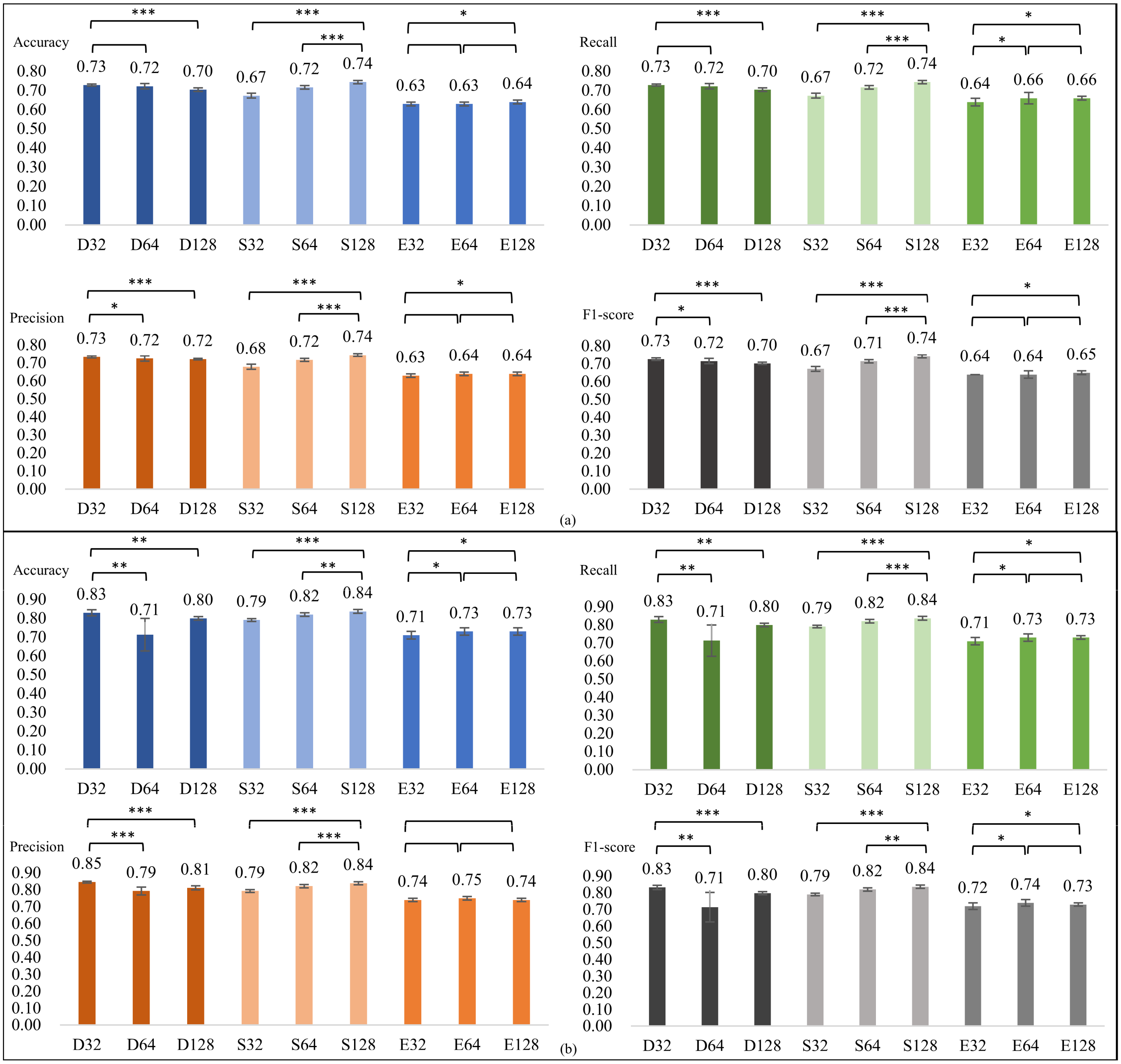

Fig. 6. For five-class (a) and four-class (b) classification, EEG data are classified using CNN model (EEGNet (E), Deep ConvNet (D) and Shallow ConvNet (S)) with different batchsize, for example, D32 = Deep ConvNet model with batchsize = 32. Asterisk indicates the significante difference, * indicates $p < 0.05$, ** indicates $p < 0.01$, and *** indicates $p < 0.001$.

cross-validation, the Deep ConvNet model with batchsize = 32 attains the optimal average classification accuracy of 73% and 83% for five- and four-class classification, respectively; the Shallow ConvNet model with batchsize = 128 attains the optimal average classification accuracy of 74% and 84% for five- and four-class classification, respectively; the EEGNet model with batchsize = 128 attains the optimal average classification accuracy of 64% and 73% for five- and four-class classification, respectively, they were chosen for further analysis. Besides, to demonstrate the advantage of the proposed SDCAN model over the existing CNN with adversarial theory models, we also applied the combination of CNN (EEGNet, Deep ConvNet, and Shallow ConvNet) models with adversarial theory to our dataset, denoted as Deep ConvNet+Ad, Shallow ConvNet+Ad, and EEGNet+Ad, respectively.

The traditional classifiers were applied to the features extracted from the theta band of recorded EEG signals according to [19], concretely, those features are the mean and variance of PSD of each channel, the difference between the absolute power of asymmetric channels of the left and right hemisphere of the brain (divisional asymmetry), the ratio between the absolute power of asymmetric channels of the left and right hemisphere of the brain (rational asymmetry), and the correlation between asymmetric channels for the left and right hemispheres of the brain.

TABLE II

THE AVERAGE STRESS CLASSIFICATION PERFORMANCE OF DIFFERENT MODEL ON TEST SET FOR FIVE-CLASS AND FOUR-CLASS CLASSIFICATION. DC = DEEP CONVNET MODEL, SC = SHALLOW CONVNET MODEL, EN+AD = EEGNET WITH ADVERSARIAL THEORY, DC+AD = DEEP CONVNET WITH ADVERSARIAL THEORY, SC+AD = SHALLOW CONVNET WITH ADVERSARIAL THEORY, SVM = SUPPORT VECTOR MACHINE, LDA = LINEAR DISCRIMINANT ANALYSIS. ALL RESULTS WERE PRESENTED AS MEAN ± STD AFTER 10-FOLD CROSS-VALIDATION

Models	Five-class classification				Four-class classification			
	Accuracy(%)	Precision(%)	Recall(%)	F1-score(%)	Accuracy(%)	Precision(%)	Recall(%)	F1-score(%)
EEGNet	63.69±1.00	64.20±1.48	72.83±1.29	64.87±0.97	72.96±0.98	74.18±1.00	72.56±0.98	73.19±0.87
Deep ConvNet	72.83±0.55	73.45±0.55	72.83±0.55	72.56±0.74	82.93±1.65	84.60±0.53	82.43±1.60	83.25±1.32
Shallow ConvNet*	74.37±0.86	74.45±0.74	74.37±0.86	74.18±0.86	83.65±1.02	83.86±0.88	83.55±1.02	83.63±0.99
EEGNet + Ad	59.46±2.13	60.29±1.91	59.82±2.11	58.11±2.90	73.76±1.32	74.10±1.44	73.93±1.35	73.86±1.67
Deep ConvNet + Ad	60.38±8.59	70.94±3.09	59.03±13.7	60.00±12.9	74.72±0.61	79.78±1.47	75.19±0.63	75.39±5.98
Shallow ConvNet +Ad	51.50±3.74	61.22±3.01	54.27±5.33	51.10±7.50	70.49±3.04	75.09±2.31	71.24±3.80	70.36±4.82
SVM	33.24±0.24	30.45±0.35.	33.17±0.25	27.52±0.51	43.01±0.12	42.36±0.21	42.90±0.22	40.39±0.32
LDA	31.61±0.15	25.35±0.19	31.40±0.14	22.67±0.21	43.89±0.11	47.82±0.12	43.81±0.21	42.06±0.21

The asterisk (*) indicates the significante difference with p < 0.05.

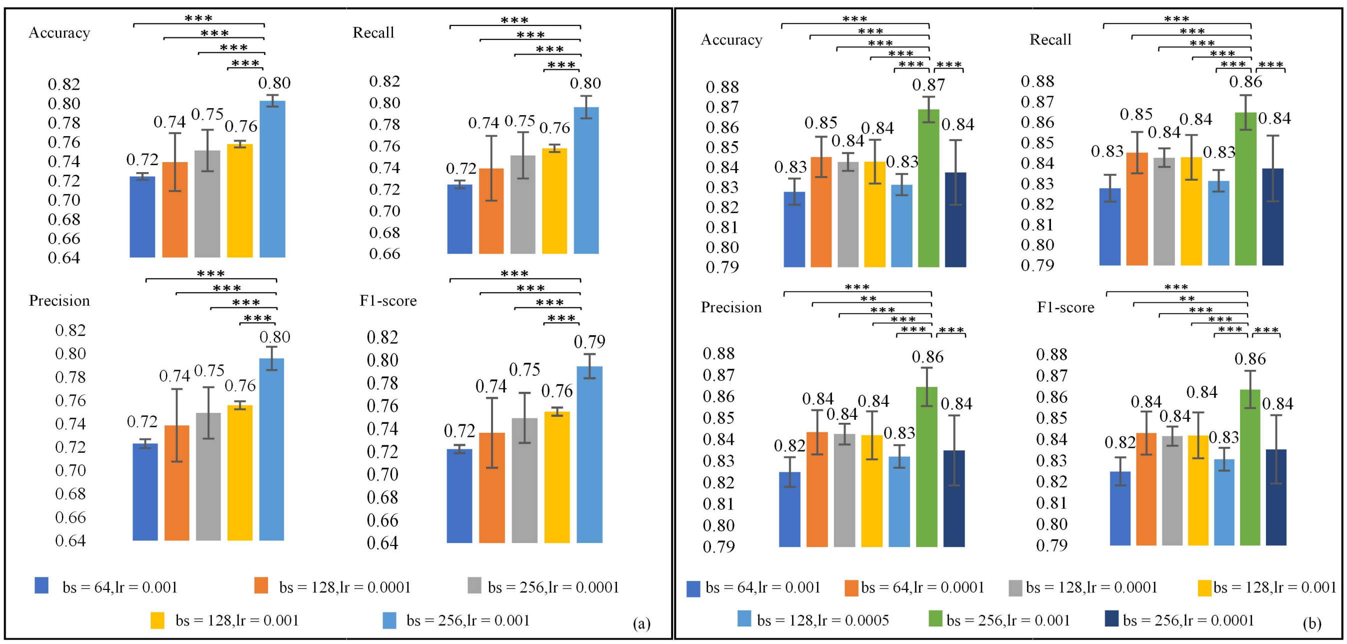

Fig. 7. For five-class (a) and four-class (b) classification, EEG signals are classified using the SDCAN model with different parameter combinations, bs = batchsize, lr = learning rate. Asterisk indicates the significante difference, * indicates $p < 0.05$, ** indicates $p < 0.01$, and *** indicates $p < 0.001$.

We demonstrate the comparison among the optimal deep learning models (i.e., EEGNet model with batchsize = 128, Deep ConvNet model with batchsize = 32, Shallow ConvNeet model with batchsize = 128), the existing CNN with adversarial theory models, and the traditional classifiers, each model performed 10-fold cross-validation for four-class and five-class classification, as shown in Table II. The comparison demonstrates that the Shallow ConvNet model with batchsize = 128 obtained the best classification among the eight models ($p < 0.05$), and deep learning models outperformed traditional classifiers, so only the deep learning methods are considered in the following analysis.

2) SDCAN: A major disadvantage of GAN is that the discriminator is unstable during training, which makes GAN easy to fall into model collapse when inappropriate parameters are chosen. For SDCAN, it is also essential for appropriate parameter setting. Four-class and five-class classification of stress stages from the collected EEG in our TSST experiment using SDCAN with combinations of a variety of batchsize and learning rate is performed and evaluated by 10-fold cross-validation. The results are shown in Fig. 7. It can be seen that the classification results of SDCAN vary greatly when different parameter combinations are chosen. The optimal average classification accuracy of 80% and 87% for five- and four-class classification, respectively, is obtained when batchsize = 256 and lr = 0.001.

D. Comparison Between Different Classifiers

Since Shallow ConvNet performs better than other models for stress states classification as shown in Section III-C-2, here we compare the detailed performance of SDCAN with Shallow ConvNet only, with results briefly summarized in Tables III

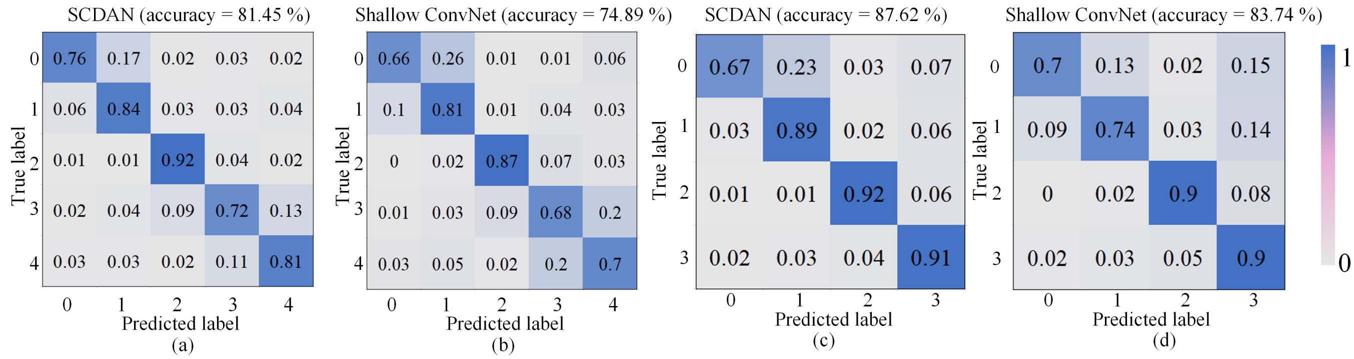

Fig. 8. For five-class classification ((a) and (b)), the confusion matrix of the best classification results of SDCAN (batchsize = 256, lr = 0.001) and Shallow ConvNet (batchsize = 128, lr = 0.001) after 10-fold cross validation. 0 represents before-stress state, 1 represents medium-stress state, 2 represents high-stress state, 3 represents the early stage of stress recovery, and 4 represents the late stage of stress recovery. For four-class classification ((c) and (d)), the confusion matrix of EEG data classification results of SDCAN (batchsize = 256, lr = 0.001) and Shallow ConvNet (batchsize = 128, lr = 0.001). 0 represents before-stress state, 1 represents medium-stress state, 2 represents high-stress state, 3 represents the stress recovery stage.

TABLE III
COMPARISON OF ACCURACY, PRECISION, RECALL AND F1-SCORE OF SDCAN MODEL AND SHALLOW CONVNET MODEL ON THE TEST SET FOR FIVE-CLASS CLASSIFICATION. ALL RESULTS WERE PRESENTED AS MEAN ± STD AFTER 10-FOLD CROSS-VALIDATION

Model	Accuracy (%)	Precision (%)	Recall (%)	F1-score (%)
Shallow ConvNet	74.37±0.86	74.44±0.74	74.37±0.86	74.13±0.86
SDGAN	80.30±0.59 ***	79.62±0.99 ***	79.60±1.05 ***	79.48±1.05 ***

The asterisk indicates the significante difference, *** indicates p < 0.001

TABLE IV
COMPARISON OF ACCURACY, PRECISION, RECALL AND F1-SCORE OF SDCAN MODEL AND SHALLOW CONVNET MODEL ON THE TEST SET FOR FOUR-CLASS CLASSIFICATION. ALL RESULTS WERE PRESENTED AS MEAN ± STD AFTER 10-FOLD CROSS-VALIDATION

Model	Accuracy (%)	Precision (%)	Recall (%)	F1-score (%)
Shallow ConvNet	83.65±1.02	83.86±0.88	83.65±1.02	83.63±0.99
SDCAN	86.89±0.64 ***	86.46±0.89 ***	86.45±0.84 ***	86.35±0.88 ***

The asterisk indicates the significante difference, *** indicates p < 0.001

and Tables IV. It can be seen that for five- and four-class classification, SDCAN performs better than Shallow ConvNet in terms of accuracy, precision, recall, and f1-score ($p < 0.001$ for each evaluation metric). The confusion matrices of the best classification result for SDCAN and Shallow ConvNet after 10-fold cross-validation are shown in Fig. 8. It can be seen that the SDCAN performs better than Shallow ConvNet in terms of accuracy for every stress level, no matter for five- or four-class classification.

E. Leave- One-Subject-Out-Cross-Validation

Cross-subject classification has always been challenging in deep learning, and the SDCAN model has the potential for good performance in this aspect due to its design principle. Here we perform LOOCV for stress states classification using EEGNet with batchsize = 128, Deep ConvNet with batchsize = 32, Shallow ConvNet with batchsize = 128, CNN with adversarial theory models, and SDCAN with optimal parameters. Moreover, We adopted the euclidean space data alignment approach (EA) proposed by He *et al.* [44] on the dataset when conducting LOOCV by the proposed SDCAN model, this approach aligns EEG trials from different subjects in the euclidean space to make them more similar and hence improve the learning performance of a new subject. The average LOOCV accuracies of four- and five-class of EA-SDCAN have been significantly improved compared with the proposed SDCAN model without EA ($p < 0.05$). The evaluation results for the overall average accuracy are shown in Table V. As shown in Table V, the average accuracy for the five-class classification obtained by the EA-SDCAN model and SDCAN model is 48.17% and 45.69%, and for the four-class classification is 60.52% and 58.91%, respectively, higher than that of the other models. An individual detailed comparison among the SDCAN model, the EA-SDCAN model, and other deep learning models is demonstrated in the appendix (Tables VIII-IX).

Our proposed SDCAN and EA-SDCAN models are also compared in terms of classification accuracy to state-of-the-art LOOCV cross-subject muli-level stress classification results in the literature, as shown in Table VI. It can be seen that our EA-SDCAN achieves 60.52% accuracy for the more difficult 4-class classification task, outperforming the reported 2-class artificial neural network (ANN), and linear discriminant analysis (LDA), slightly inferior to the 2-class support vector machine (SVM) and 3-class multilayer perceptron (MLP).

F. Feature Analysis

For analysis of the features learned by the SDCAN model and to illustrate that these features are stress-related, we did the canonical correlation analysis (CCA) [45] between two feature groups including SDCAN-based and handcraft-based features. SDCAN-based features are extracted by the proposed SDCAN model from the data of each subject at each stress

TABLE V

THE AVERAGE STRESS CLASSIFICATION PERFORMANCE OF DIFFERENT MODEL ON TEST SET FOR FIVE-CLASS AND FOUR-CLASS CLASSIFICATION BY LOOCV. DC = DEEP CONVNET MODEL, SC = SHALLOW CONVNET MODEL, EN+AD = EEGNET WITH ADVERSARIAL THEORY, DC+AD = DEEP CONVNET WITH ADVERSARIAL THEORY, SC+AD = SHALLOW CONVNET WITH ADVERSARIAL THEORY, EA = EUCLIDEAN ALIGNMENT APPROACH

Models	Five-class classification				Four-class classification			
	Accuracy(%)	Precision(%)	Recall(%)	F1-score(%)	Accuracy(%)	Precision(%)	Recall(%)	F1-score(%)
EEGNet	37.17±9.99	41.27±11.25	37.70±9.84	33.06±9.99	46.67±11.7	52.47±10.95	46.40±11.67	42.52±11.66
DC	32.56±9.51	38.03±9.52	32.51±9.41	27.58±9.20	41.66±9.85	47.87±12.44	41.63±9.82	37.08±8.63
SC	37.83±8.05	42.13±10.35	38.19±8.77	33.19±9.16	45.16±10.13	49.16±11.11	45.01±10.11	40.28±10.86
EN+Ad	37.13±10.0	41.29±11.28	37.67±9.86	32.93±10.2	46.49±11.74	51.84±11.63	46.43±11.68	42.18±11.74
DC+Ad	37.13±10.0	41.37±11.27	37.62±9.91	32.87±10.2	46.69±11.64	51.79±11.82	45.62±11.59	42.21±11.79
SC+Ad	37.12±10.0	41.25±11.42	37.62±9.91	32.80±10.3	46.76±11.62	51.92±11.81	46.69±11.57	44.23±11.78
SDCAN	45.69±4.77	47.56±10.76	45.56±4.85	41.17±5.89	58.91±7.18	53.50±9.05	58.69±7.33	52.86±7.69
EA-SDCAN	**48.17±3.37**	**49.60±9.12**	**47.90±3.52**	**42.54±3.60**	**60.52±6.14**	**54.17±5.40**	**60.54±6.14**	**54.07±6.37**

TABLE VI

COMPARISON OF CLASSIFICATION PERFORMANCE BY LOOCV MANNER

Model	Number of subjects	Feature extration	Number of class	Accuracy (%)
MLP [19]	28	Yes	3-class	64.28
SVM [42]	28	Yes	2-class	67.92
ANN [43]	25	Yes	2-class	44.00
LDA [43]	25	Yes	2-class	60.00
SDCAN	21	No	4-class	58.91
EA-SDCAN	21	No	4-class	60.52

MLP = Multilayer Perceptron, SVM = Support Vector Machine, ANN = Artificial Neural Network, LDA = Linear Discriminant Analysis

stage, they are the output of the layer before the classification layer of the discriminative network. Handcraft-based features include five sub-feature sets that are extracted from the theta band of each channel of the recorded EEG data, and they have been proved to be stress-related and applied for stress level classification by [19]. These included the mean and variance of PSD of each channel, the divisional asymmetry, the rational asymmetry, and the correlation between asymmetric channels for the left and right hemispheres of the brain.

The r-value of CCA between the SDCAN-based features and each sub-feature set in handcraft-based features is shown in Table VII. The first six columns demonstrate the correlation and significance between network feature at each stress stage and one of the sub-feature sets of the handcraft-based features, the last column shows the correlation and significance between network feature from each stress stage and the combination of the handcraft-based features. The last row in Table VII gives the chance level between SDCAN-based features and random white noise.

As we can see from Table VII, after the CCA analysis, the r-value between the SDCAN-based features and the combination of handcraft-based features shows a high correlation (r-value ranging from 0.61 to 0.94) and significance ($p < 0.001$), and they are all higher than the chance level, demonstrating the features learned by the SDCAN model are correlated to stress-related features in EEG. Besides, the r-values between the SDCAN-based features and the feature of correlation are around 0.9, showing the possibility that the features learned by the proposed SDCAN model are highly correlated to the correlation of asymmetric channels for the left and right hemispheres of the brain. The results of the CCA analysis prove that the SDCAN model learned the stress-related features from raw EEG.

IV. DISCUSSION

This paper proposes a framework for the end-to-end classification of perceived mental stress at multiple levels using EEG data. For this purpose, a modified experimental paradigm based on TSST is designed to induce multiple-level mental stress. EEG is monitored and salivary cortisol is used for mental stress stages calibration. A novel classification model that combines CNN with adversarial inference is proposed to recognize mental stress. The results indicate that it is feasible to make an end-to-end model that can detect mental stress and discriminate between different stages of stress. Moreover, the adversarial inference contributes to subject-invariant features extraction, which leads to better generalization across subjects compared with traditional networks. Compared to the existing CNN with adversarial theory models, the technical advantage of the proposed SDCAN model is that we constructed two symmetric networks, including a discriminative network, and a generative network, to automatically capture invariant and discriminative features from EEG. The generative network works as a feature extractor and outputs the generative data which are used as one additional class for classification. In contrast, the existing CNN+adversarial theory methods do not generate data. By outputting the generated data, our model can disentangle specific attributes from the data, and finer attributes can be learned to improve classification accuracy with the iteration of training. Statistic results proved the proposed SDCAN model significantly outperforms the existing CNN with adversarial theory models.

For the classification framework, the SDCAN model is proposed in this work. Two types of classification were performed, with one as LOOCV, and the other as data mixing from all subjects. The principle of LOOCV is to guarantee that the subject used for testing cannot be mixed into the training sets to guarantee no data leakage. For the second type of classification, data mixed from all subjects were then divided into training, validation, and test sets, where the test

TABLE VII
THE r-VALUE OF CCA BETWEEN THE PROPOSED SDCAN MODEL FEATURES AT EACH STRESS STAGES AND THE FEATURES CALCULATED FROM THE RECORED EEG DATA

	Bandpower	Mean of PSD	Variance of PSD	Divisional asymmetry	Aational asymmetry	Correlation	The combination of handcraft-based features
Before stress	0.79***	0.74***	0.74***	0.68***	0.65***	0.92***	0.80***
Medium stress	0.88***	0.87***	0.85***	0.90***	0.90***	0.92***	0.89***
High stress	0.94***	0.95***	0.93***	0.94***	0.91***	0.91***	0.94***
Recovery	0.57***	0.58***	0.55***	0.57***	0.57***	0.89***	0.61***
Chance level	0.34±0.01	0.30±0.01	0.29±0.04	0.29±0.04	0.28±0.04	0.28±0.04	0.28±0.09

PSD = power spectral density. The asterisk indicates the significante difference, *** indicates $p < 0.001$

set was not strictly consisted of unseen subjects. As depicted in a previous study [46], these two types of data division should be built for different purposes and goals. Applying LOOCV is appropriate for the general population. The mixed-data division-based user-independent classification is restricted to applications where only a specific population is considered, with training and subsequent classification tasks performed on the same specific population but not a general population. Such user-independent classification and data division strategy has been applied in many studies of stress classification [19], [47], [48]. It can be designed for a specific population who is suffering from stress-related mental illness and is appropriate for real-life personalized stress state detection applications when the algorithm is utilized in portable stress detecting equipment.

The adversarial theory applied to the SDCAN model is commonly used in domain adaptation in transfer learning [49], it can learn subject-invariant representations which make cross-subject learning possible. While it is challenging to achieve good cross-subject multi-level stress classification due to the variability of EEG signals among individuals, as shown in Table VI, the two-class and three-class classifications of LOOCV range from 44% to 67%. In contrast, our proposed SDCAN and EA-SDCAN achieve an average accuracy of 58.91% and 60.52% for four-class classification, respectively, which is comparable to most state-of-the-art results for much easier two- and three-class stress level classification tasks, and much higher than chance accuracy of 25%. For the more difficult five-class classification, our average accuracy decreases to 48.17%, but still much higher than the chance accuracy of 20%. In summary, this study obtains reasonably acceptable accuracy for cross-object multilevel stress classification, but there is still much room for improvement.

In the framework of GAN, the generator mimics the distribution of real data due to its outstanding feature extracting ability. In the SDCAN model, the generator extracts certain features from every class of real data which are non-redundant and consistent, so the generated data in this paper can help the discriminator to classify the K-class of the original EEG and achieve good generalization results across subjects. In this work, the parameters of the generator are updated once after the parameters of the discriminator are updated five times, which indicates that after the generator is updated once, there was a batch of generated data. The main objective of this work is to improve the classification ability of the discriminator, so we do not pay attention to the quality of generated data.

For the labeling of mental stress, first, it can be observed from Fig.5 (a) that during the whole recovery stage, cortisol level is in the same range as the medium stress state during TSST, but we denote the stages of stress according to the changing trend of salivary cortisol concentration values instead of only by the specific value of cortisol concentration. During the procedure of TSST, we were unable to collect saliva samples during the speech period, but according to [50], the cortisol secretion rate ascend to its peak within a short time window after speech period onset, which means the changing trend of cortisol concentration varies between the recovery stage and medium stress state. The low FN of the medium stress state and the recovery state in the confusion matrices from Fig. 8 indicates dividing the medium stress state and the recovery state as two different stress stages is correct. Second, due to the obvious descending trend of salivary cortisol concentration values during the 20 minutes after TSST, it is reasonable to assume that for the stress recovery stage, there are differences between the first 10 minutes after stress stimulation immediately and the last 10 minutes, research [4] also indicated that the effect size of cortisol within 20 minutes from stressor termination changes significantly, so the analysis is conducted for two cases: (1) mental stress-related EEG data is divided into four stages including two stress states (the medium-stress state and the high-stress state), before stress state, and stress recovery state, (2) the stress recovery state is further divided into the early stress recovery state and the late stress recovery state. The classification results of EEG verify our assumption. The proposed SDCAN model achieves 87.62% and 81.45% accuracy for four- and five-class classification, respectively, and for the five-class classification after 10-fold cross-validation as shown in Fig. 8, the TP and FN of the label 3 and label 4 verify that the early recovery and late recovery can be distinguished.

There are also some practical considerations when we conducted five- and four-class classification. Different levels of stress have different effects on the human body. It is helpful to classify stress into multistage stress for the prevention, follow-up, and prognosis of recovery from stress-stimulation-related psychiatric disorders. High levels of stress can be harmful to human health, but moderate levels of mild stress can sometimes be effective in helping people get more concentration,

TABLE VIII
COMPARISON RESULTS OF EACH SUBJECT BEFORE AND AFTER THE APPLICATION OF EA APPROACH

Sub	Models	Five-class classification				Four-class classification			
		Accuracy (%)	Precision (%)	Recall (%)	F1-score (%)	Accuracy (%)	Precision (%)	Recall (%)	F1-score (%)
S2	EA-SDCAN	48.67	50.68	48.67	42.55	63.00	56.19	63.37	58.20
	SDCAN	**48.40**	**51.71**	**48.38**	**49.25**	**62.19**	**53.67**	**61.48**	**56.13**
S3	EA-SDCAN	47.72	38.34	47.72	43.95	61.17	57.35	61.17	53.38
	SDCAN	**40.00**	**38.48**	**40.69**	**37.71**	**60.47**	**51.95**	**61.09**	**56.13**
S4	EA-SDCAN	49.92	46.73	49.92	46.73	67.33	54.33	67.33	59.88
	SDCAN	**46.83**	**48.35**	**46.83**	**42.53**	**57.96**	**54.20**	**52.96**	**52.67**
S5	EA-SDCAN	42.44	46.76	42.44	36.36	57.13	49.84	57.13	46.02
	SDCAN	**40.23**	**37.34**	**39.16**	**37.65**	**52.96**	**54.20**	**52.96**	**48.50**
S6	EA-SDCAN	46.16	49.02	46.17	43.95	61.17	57.35	61.17	53.38
	SDCAN	**45.67**	**42.28**	**45.63**	**41.98**	**59.77**	**53.12**	**59.53**	**52.45**
S7	EA-SDCAN	50.07	52.40	50.07	43.19	68.00	54.96	68.00	60.31
	SDCAN	**51.27**	**51.79**	**51.26**	**44.48**	**65.06**	**59.98**	**65.06**	**59.37**
S8	EA-SDCAN	45.00	45.36	45.61	40.90	69.20	58.27	69.20	57.34
	SDCAN	**43.13**	**37.75**	**42.89**	**36.63**	**68.59**	**58.28**	**68.20**	**62.06**
S9	EA-SDCAN	46.08	44.24	46.08	39.24	55.60	54.54	55.60	54.61
	SDCAN	**42.40**	**48.45**	**42.40**	**40.78**	**51.80**	**55.06**	**52.50**	**45.17**
S10	EA-SDCAN	48.83	59.24	49.83	44.96	48.67	43.68	48.67	42.55
	SDCAN	**45.95**	**61.12**	**45.95**	**41.04**	**45.33**	**44.52**	**45.33**	**39.36**
S11	EA-SDCAN	48.67	40.61	48.67	48.33	63.75	63.63	63.75	63.30
	SDCAN	**47.50**	**41.83**	**45.39**	**41.99**	**63.43**	**73.35**	**63.36**	**54.21**
S12	EA-SDCAN	52.67	51.71	52.67	47.98	58.83	49.39	58.83	49.95
	SDCAN	**50.28**	**51.38**	**50.28**	**47.84**	**51.53**	**49.90**	**51.53**	**48.80**
S13	EA-SDCAN	48.33	40.34	52.68	44.92	53.17	51.45	53.17	49.00
	SDCAN	**45.31**	**39.53**	**45.16**	**35.80**	**52.81**	**47.17**	**52.89**	**49.20**
S14	EA-SDCAN	42.08	51.25	42.08	36.51	54.08	54.36	54.08	49.15
	SDCAN	**41.18**	**45.63**	**41.09**	**35.93**	**51.56**	**42.14**	**49.69**	**44.58**
S15	EA-SDCAN	53.93	55.29	53.93	42.46	66.58	57.25	66.58	56.60
	SDCAN	**53.91**	**58.81**	**54.38**	**49.32**	**67.74**	**51.07**	**67.73**	**57.85**
S16	EA-SDCAN	47.42	47.98	47.42	36.62	57.67	49.17	57.67	47.76
	SDCAN	**38.91**	**34.37**	**38.67**	**33.65**	**68.64**	**71.50**	**68.64**	**67.70**
S17	EA-SDCAN	47.50	45.49	47.96	41.53	57.33	53.10	57.33	45.15
	SDCAN	**51.53**	**49.90**	**51.53**	**48.80**	**64.72**	**61.64**	**64.72**	**61.8**
S18	EA-SDCAN	48.00	49.94	48.00	42.82	64.83	59.44	64.83	63.06
	SDCAN	**41.82**	**45.42**	**41.82**	**40.32**	**64.45**	**57.18**	**65.16**	**60.52**
S19	EA-SDCAN	44.00	54.63	44.00	41.64	50.42	42.25	50.42	46.80
	SDCAN	**40.14**	**54.42**	**40.14**	**35.41**	**48.67**	**44.93**	**49.14**	**44.93**
S20	EA-SDCAN	55.67	55.37	51.67	51.77	68.75	63.28	68.75	63.35
	SDCAN	**55.40**	**55.17**	**55.40**	**51.39**	**62.03**	**56.65**	**62.73**	**53.89**
S21	EA-SDCAN	49.67	36.37	41.14	31.77	66.25	52.36	66.25	58.27
	SDCAN	**45.70**	**27.92**	**45.70**	**29.13**	**65.63**	**49.54**	**65.70**	**56.48**
S22	EA-SDCAN	49.08	79.78	49.08	43.17	58.00	55.37	58.00	57.31
	SDCAN	**43.96**	**77.02**	**43.96**	**42.90**	**51.72**	**33.48**	**52.03**	**38.33**

and a more accurate grasp of the degree of recovery from stress can also help people regulate their emotions more effectively to maintain mental health. We hope to provide full monitoring of stress-related mental illnesses and accurate stress regulation when this research comes into practice.

With aspect to the saliva sampling interval, according to the pharmacological theory brought out by research [4], [50], the amount of time for the cortisol conversion process differs among individuals, and the conversion relies on multiple conditions such as the secretion of cholesterol, so the whole conversion process of the glucocorticoid such as cortisol requires 10–15 min [51]. So Linares *et al.* [52] suggested that repeated salivary samples should be collected at 10-15 min intervals. Furthermore, previous research focusing on TSST experiments [53], [54] commonly considered the cortisol changes as the 10-minute interval. Another consideration is that sampling should not influence the subject's stress level, which means the action of taking saliva samples need to cost a minimal mental and physical burden for the participants [55], and for this reason, we conducted a pre-experiment and all participants reflected no stressful feelings for the 10-minute salivary sampling interval. So in this study, the saliva samples

TABLE IX

STRESS CLASSIFICATION PERFORMANCE OF DIFFERENT MODEL FOR FIVE-CLASS AND FOUR-CLASS CLASSIFICATION BY LOOCVON SUBJECT 2-SUJECT 9. DC = DEEP CONVNET MODEL, SC = SHALLOW CONVNET MODEL, EN+AD = EEGNET WITH ADVERSARIAL THEORY, DC+AD = DEEP CONVNET WITH ADVERSARIAL THEORY, SC+AD = SHALLOW CONVNET WITH ADVERSARIAL THEORY

Subject	Models	Five-class classification Accuracy (%)	Precision (%)	Recall (%)	F1-score (%)	Four-class classification Accuracy (%)	Precision (%)	Recall (%)	F1-score (%)
S2	EEGNet	25.14	31.57	25.14	22.24	36.80	38.90	36.80	37.09
	DC	22.41	34.33	22.42	18.13	39.67	51.37	39.68	32.48
	SC	34.48	32.09	34.49	27.92	50.79	51.14	50.78	47.32
	EN+Ad	29.24	34.81	29.09	29.34	35.19	40.19	35.58	36.45
	DC+Ad	28.94	33.94	28.74	29.83	39.06	41.77	38.89	32.98
	SC+Ad	21.65	26.04	21.48	20.68	48.66	40.44	48.28	34.04
	SDCAN	**48.67**	**50.68**	**48.67**	**42.25**	**63.00**	**56.19**	**63.37**	**58.20**
S3	EEGNet	30.98	31.38	30.98	26.78	42.37	46.59	42.37	39.69
	DC	29.06	40.68	29.06	25.80	41.82	45.42	41.82	40.32
	SC	32.49	39.93	32.48	28.48	47.78	44.76	47.77	45.52
	EN+Ad	28.55	31.58	24.67	20.86	28.41	44.50	28.95	31.55
	DC+Ad	33.24	30.45	33.17	27.52	38.71	40.54	38.47	38.18
	SC+Ad	35.87	28.16	36.26	31.52	43.18	43.70	43.05	40.31
	SDCAN	**47.72**	**38.34**	**47.72**	**43.95**	**61.17**	**57.35**	**61.17**	**53.38**
S4	EEGNet	37.22	42.31	37.22	33.29	50.62	50.02	50.62	47.46
	DC	35.76	36.39	35.77	32.60	42.33	44.35	42.32	37.97
	SC	43.28	44.44	42.42	41.61	43.44	42.38	42.73	39.41
	EN+Ad	37.35	37.35	37.36	30.12	54.69	53.20	54.33	53.19
	DC+Ad	44.57	41.95	44.57	37.59	48.29	44.25	48.58	44.97
	SC+Ad	41.52	43.47	41.30	41.29	49.85	50.29	49.74	49.83
	SDCAN	**49.92**	**46.73**	**49.92**	**46.73**	**67.33**	**54.35**	**67.33**	**59.88**
S5	EEGNet	42.14	37.14	42.14	38.34	39.89	58.00	39.89	35.52
	DC	29.33	34.09	29.34	23.98	48.81	53.50	48.81	47.54
	SC	37.81	40.11	37.80	35.81	45.61	37.45	44.04	34.74
	EN+Ad	37.78	34.80	38.34	32.72	43.84	52.13	44.22	43.64
	DC+Ad	29.04	34.85	29.89	27.12	56.16	49.16	56.40	50.87
	SC+Ad	30.06	29.40	30.30	22.87	46.60	41.67	46.60	43.28
	SDCAN	**42.44**	**46.76**	**42.44**	**36.36**	**57.13**	**49.84**	**57.13**	**46.02**
S6	EEGNet	36.85	36.80	36.85	32.97	40.04	50.11	40.04	34.98
	DC	35.03	28.67	35.02	23.85	39.48	43.40	39.48	36.38
	SC	35.94	31.61	35.93	27.11	26.97	27.25	26.97	15.84
	EN+Ad	36.29	32.90	36.15	26.28	43.54	45.80	43.61	39.91
	DC+Ad	31.61	25.35	31.40	22.67	28.05	37.84	28.23	19.79
	SC+Ad	34.23	40.45	34.27	30.35	41.19	41.58	41.16	39.12
	SDCAN	**46.16**	**49.02**	**46.17**	**43.95**	**61.17**	**57.35**	**61.17**	**53.38**
S7	EEGNet	48.54	48.24	48.53	40.38	58.12	70.93	58.12	51.02
	DC	44.38	45.71	44.37	36.08	51.56	55.14	51.56	47.73
	SC	43.55	39.34	42.19	36.86	58.20	54.81	56.45	52.76
	EN+Ad	35.74	53.39	35.80	30.66	47.85	47.96	47.99	41.36
	DC+Ad	44.99	37.49	42.05	34.71	54.10	53.90	54.16	51.62
	SC+Ad	40.76	51.49	40.68	35.63	55.08	54.28	55.13	54.50
	SDCAN	**50.07**	**52.40**	**50.07**	**43.19**	**68.00**	**54.96**	**68.00**	**60.31**
S8	EEGNet	40.14	43.74	40.14	35.59	56.30	53.35	56.30	50.93
	DC	43.82	51.08	43.82	39.61	61.81	60.92	61.81	54.97
	SC	37.91	47.13	37.91	34.05	59.51	59.41	59.51	49.11
	EN+Ad	45.65	48.72	51.51	47.66	60.73	61.83	61.02	52.48
	DC+Ad	42.05	37.49	42.05	34.71	41.58	61.13	41.54	34.35
	SC+Ad	35.05	47.79	35.15	34.40	37.50	51.30	37.20	32.13
	SDCAN	**45.00**	**45.36**	**45.61**	**40.90**	**69.20**	**58.27**	**69.20**	**57.34**
S9	EEGNet	43.48	48.70	43.48	42.82	39.93	51.68	39.93	38.16
	DC	32.11	45.23	32.11	26.18	41.06	54.71	41.06	39.21
	SC	38.52	30.02	38.44	30.10	39.16	55.73	39.16	38.07
	EN+Ad	32.37	48.43	39.52	39.03	43.60	50.52	43.31	40.23
	DC+Ad	30.06	40.44	30.02	24.47	43.90	47.82	43.81	42.06
	SC+Ad	32.81	39.08	32.83	28.76	36.61	47.32	36.33	33.14
	SDCAN	**46.08**	**44.24**	**46.08**	**39.24**	**55.60**	**54.54**	**55.60**	**54.61**
S10	EEGNet	39.08	46.46	39.09	36.58	38.11	53.35	38.11	40.38
	DC	23.02	35.94	23.02	19.76	41.06	54.71	41.06	39.21
	SC	39.02	54.14	39.01	37.48	39.16	55.73	39.16	38.07
	EN+Ad	38.38	47.16	38.43	35.59	43.75	51.95	43.94	41.73
	DC+Ad	35.12	47.13	34.75	32.62	37.23	49.35	37.52	35.56
	SC+Ad	32.74	44.31	32.52	34.60	43.75	52.93	43.55	39.41
	SDCAN	**48.83**	**59.64**	**49.83**	**44.96**	**48.67**	**43.68**	**48.67**	**42.55**

DC = Deep ConvNet, SC = Shallow ConvNet, EN = EEGNet, Ad = adversarial theory

TABLE IX

(Continued.) STRESS CLASSIFICATION PERFORMANCE OF DIFFERENT MODEL FOR FIVE-CLASS AND FOUR-CLASS CLASSIFICATION BY LOOCVON SUBJECT 11-SUJECT 19. DC = DEEP CONVNET MODEL, SC = SHALLOW CONVNET MODEL, EN+AD = EEGNET WITH ADVERSARIAL THEORY, DC+AD = DEEP CONVNET WITH ADVERSARIAL THEORY, SC+AD = SHALLOW CONVNET WITH ADVERSARIAL THEORY

Subject	Models	Five-class classification Accuracy (%)	Precision (%)	Recall (%)	F1-score (%)	Four-class classification Accuracy (%)	Precision (%)	Recall (%)	F1-score (%)
S11	EEGNet	30.47	28.98	30.47	25.79	38.20	46.60	38.20	33.94
	DC	20.98	25.66	20.98	18.62	18.27	22.64	18.27	16.46
	SC	21.05	33.79	21.05	20.81	24.50	35.34	24.44	22.85
	EN+Ad	18.32	16.77	18.21	14.01	22.37	24.07	22.42	18.35
	DC+Ad	11.29	24.36	24.79	21.63	13.14	21.26	13.29	13.00
	SC+Ad	12.29	17.96	23.26	13.54	17.97	19.06	18.34	17.16
	SDCAN	**48.67**	**40.61**	**48.67**	**48.33**	**63.75**	**63.63**	**63.75**	**63.30**
S12	EEGNet	29.68	43.47	29.68	29.50	36.31	62.74	36.31	36.81
	DC	36.82	47.86	36.82	37.44	45.95	61.12	45.95	41.04
	SC	49.14	54.48	50.47	48.76	46.43	59.56	46.43	48.56
	EN+Ad	31.11	36.32	30.86	25.88	38.99	52.72	38.67	39.63
	DC+Ad	41.76	43.51	46.74	42.86	45.53	65.12	45.60	43.00
	SC+Ad	31.18	46.38	31.14	30.77	42.68	57.49	42.90	42.57
	SDCAN	**52.67**	**51.71**	**52.67**	**47.98**	**58.83**	**49.39**	**58.83**	**49.95**
S13	EEGNet	65.57	65.78	49.34	41.60	49.60	49.17	49.60	46.71
	DC	30.32	35.50	30.32	28.47	22.58	32.40	22.57	21.77
	SC	38.78	42.60	38.78	37.68	41.59	44.71	41.59	42.06
	EN+Ad	24.85	30.03	24.56	22.58	52.34	65.18	52.07	61.80
	DC+Ad	26.93	31.30	26.97	22.45	43.01	42.36	42.90	40.39
	SC+Ad	27.83	28.52	27.84	27.54	40.43	41.64	40.42	39.66
	SDCAN	**48.33**	**40.34**	**52.68**	**44.92**	**53.17**	**51.45**	**53.17**	**49.00**
S14	EEGNet	49.34	65.78	49.34	41.60	50.76	72.08	50.76	43.14
	DC	45.33	44.52	45.33	39.36	37.48	50.98	37.48	39.26
	SC	37.58	37.81	37.57	28.04	41.77	57.63	41.77	35.22
	EN+Ad	42.47	55.63	42.42	35.14	47.77	51.05	48.07	41.21
	DC+Ad	33.45	33.26	33.63	25.97	34.66	49.70	34.92	29.44
	SC+Ad	45.31	43.85	45.47	38.42	49.43	58.05	49.44	46.46
	SDCAN	**42.08**	**51.25**	**42.08**	**36.15**	**54.08**	**54.36**	**54.08**	**49.15**
S15	EEGNet	55.32	55.67	55.32	50.48	58.09	67.29	58.09	57.32
	DC	49.61	50.96	49.61	42.42	51.95	46.03	51.33	42.10
	SC	52.75	52.76	52.75	49.02	63.65	57.85	63.65	59.00
	EN+Ad	51.49	55.89	51.03	48.73	65.40	61.48	65.07	61.80
	DC+Ad	46.21	48.47	46.18	39.99	65.55	68.01	65.36	65.97
	SC+Ad	48.66	50.83	48.82	43.88	60.19	67.74	60.16	60.80
	SDCAN	**53.93**	**55.29**	**53.93**	**42.46**	**66.58**	**57.25**	**66.58**	**56.60**
S16	EEGNet	42.40	42.20	42.39	37.02	58.70	51.83	58.70	51.18
	DC	28.84	35.27	28.93	23.69	50.00	44.49	50.01	37.97
	SC	38.83	50.48	38.83	35.41	50.50	57.56	50.50	41.44
	EN+Ad	42.86	53.98	46.25	40.81	61.38	63.11	61.41	55.83
	DC+Ad	30.51	35.47	30.12	21.44	47.84	51.91	48.00	37.22
	SC+Ad	39.51	55.14	39.19	36.14	50.07	43.79	50.00	42.53
	SDCAN	**47.42**	**47.98**	**47.42**	**36.62**	**57.67**	**49.17**	**57.67**	**47.76**
S17	EEGNet	47.59	56.43	47.59	44.74	39.96	74.87	39.96	35.45
	DC	47.11	38.13	45.86	40.61	43.96	77.02	43.96	42.90
	SC	49.22	53.05	49.22	46.59	57.81	49.44	58.83	53.48
	EN+Ad	47.55	50.46	47.52	42.19	67.26	74.57	67.30	63.62
	DC+Ad	44.90	68.37	62.86	60.00	35.67	71.27	35.69	31.19
	SC+Ad	51.49	57.34	51.53	51.18	59.85	60.82	59.84	56.62
	SDCAN	**47.50**	**45.49**	**47.96**	**41.53**	**57.33**	**53.10**	**57.33**	**45.15**
S18	EEGNet	18.14	14.41	18.14	15.86	55.17	66.91	55.17	46.68
	DC	14.21	9.14	14.21	9.39	48.32	34.14	48.32	38.19
	SC	25.86	18.81	25.56	19.57	42.26	51.61	42.26	33.92
	EN+Ad	27.16	34.99	33.57	27.77	43.23	56.45	43.33	35.18
	DC+Ad	13.47	10.88	13.57	11.85	28.05	44.63	28.62	22.60
	SC+Ad	21.50	33.13	21.50	17.19	30.28	46.48	30.54	24.76
	SDCAN	**48.00**	**49.94**	**48.00**	**42.82**	**64.83**	**59.44**	**64.83**	**63.06**
S19	EEGNet	33.15	43.08	33.14	29.82	39.79	46.13	39.79	30.63
	DC	27.46	44.46	27.46	25.37	30.25	50.26	30.25	31.42
	SC	25.35	31.72	25.35	18.76	30.67	50.36	30.67	27.53
	EN+Ad	20.81	34.07	20.72	18.00	26.28	48.74	26.18	24.06
	DC+Ad	34.59	54.97	48.81	44.24	33.52	47.68	33.54	28.78
	SC+Ad	13.21	24.20	13.13	4.62	42.90	62.71	42.67	44.73
	SDCAN	**44.00**	**54.63**	**44.00**	**41.64**	**50.42**	**42.25**	**50.42**	**46.80**

DC = Deep ConvNet, SC = Shallow ConvNet, EN = EEGNet, Ad = adversarial theory

TABLE IX

(Continued.) Stress Classification Performance of Different Model For Five-Class And Four-Class Classification by LOOCVon Subject 20-Suject 22. DC = Deep ConvNet Model, SC = Shallow ConvNet Model, EN+AD = EEGNet With Adversarial Theory, DC+AD = Deep ConvNet With Adversarial Theory, SC+AD = Shallow Convnet With Adversarial Theory

Subject	Models	Five-class classification Accuracy (%)	Precision (%)	Recall (%)	F1-score (%)	Four-class classification Accuracy (%)	Precision (%)	Recall (%)	F1-score (%)
S20	EEGNet	47.36	46.75	47.35	42.81	70.06	69.87	70.06	67.34
	DC	34.33	38.48	34.33	30.73	36.14	37.95	36.14	32.43
	SC	45.95	61.18	54.94	41.04	50.15	58.35	50.15	52.29
	EN+Ad	36.17	53.03	48.20	47.29	51.09	57.80	51.15	48.17
	DC+Ad	48.91	54.97	48.81	44.24	62.66	74.42	62.25	59.94
	SC+Ad	46.33	40.54	46.44	38.73	67.11	74.76	67.00	63.28
	SDCAN	**55.67**	**55.37**	**51.67**	**51.77**	**68.75**	**63.28**	**68.75**	**63.35**
S21	EEGNet	38.10	35.14	38.10	28.22	39.45	61.72	39.45	30.63
	DC	31.64	43.46	31.64	22.71	36.56	56.83	36.56	30.26
	SC	36.73	47.95	36.73	30.04	42.75	60.50	42.75	40.06
	EN+Ad	43.32	44.34	42.37	35.24	41.48	59.49	41.10	35.20
	DC+Ad	26.42	21.79	26.27	17.36	29.90	62.08	29.83	20.20
	SC+Ad	40.41	49.80	40.44	31.78	37.00	62.94	37.11	28.17
	SDCAN	**49.67**	**36.37**	**41.14**	**31.77**	**66.25**	**52.36**	**66.25**	**58.27**
S22	EEGNet	26.98	23.15	26.98	16.33	55.91	61.04	55.91	50.19
	DC	22.28	33.17	22.28	14.31	45.70	27.92	45.70	29.13
	SC	30.13	41.29	30.13	21.85	45.63	20.86	45.63	28.63
	EN+Ad	24.93	26.16	25.01	13.51	40.13	24.01	40.03	28.38
	DC+Ad	28.69	45.23	23.27	21.32	45.67	25.75	45.49	29.51
	SC+Ad	27.63	18.15	27.61	19.85	47.59	60.68	47.80	35.64
	SDCAN	**49.08**	**79.78**	**49.08**	**43.17**	**58.00**	**55.37**	**58.00**	**57.31**

DC = Deep ConvNet, SC = Shallow ConvNet, EN = EEGNet, Ad = adversarial theory

are collected at 10-minute sampling intervals. The previous study indicated that the stress state of human beings is a slowly changing process and maintains stability unless induced by external stimuli [56]. In this study, the subjects stayed in a stable and quiet environment throughout the experiment. Induction of stress is rigorously controlled by TSST to guarantee consistency during each experimental stage.

Various experimental tasks [57]–[59] have been used for the induction of mental stress in experimental conditions. However, whether these tasks can induce stress has been neither validated nor discussed in these studies due to their complexity and the long analysis time dictated by biological samples. The most commonly used paradigms include the Maastricht acute stress test task [57] and the Stroop task [58], as well as the socially evaluated cold pressor test [59]. Among those tasks, the validation that the achieved results in the presented studies are due to the induction of stress is unanswered. Applying TSST to induce stress has previously been demonstrated in [54], where the trend of salivary cortisol concentration is similar to what we obtain in this paper, confirming the capability of the paradigm proposed by this work to induce stress in the participants.

Even though cortisol works as the body's stress index hormone and can provide a calibration standard for stress levels, it lacks practical applications for real-time stress level monitoring as compared with EEG, on the one hand, cortisol cannot provide instantaneous stress indication due to the long conversion process, and on the other hand, the procedure of salivary cortisol detection is very complicated and time-consuming, which is further hampered by the limitations on proper temperature and other conditions required by the storage of saliva before laboratory measurements. Thanks to recent advancements, compact lightweight devices such as MindWave Mobile Headset [15] and Muse [16] are used in studies related to detecting mental stress. These types of EEG equipment have been on the market for the people who need to monitor stress levels to allow a more consumer-friendly means to monitor brain activities and real-time stress levels detection.

A limitation of this work is that the network proposed in this paper extracts most features automatically from only the frequency domain. In the future, we can pay more attention to the time-domain of EEG signals and combine the SDCAN model with models such as LSTM, and even achieve the online classification.

V. Conclusion

This paper aims to present a robust and end-to-end stress recognition method from high-dimensional EEG signals. We proposed a novel network named SDCAN, and the results show that the SDCAN significantly outperforms the existing CNN for stress state classification from EEG with an average accuracy of 86.89% and 80.30% for four- and five-class, respectively. Additionally, the SDCAN is further compared with the existing CNN by LOOCV, and the results show that the SDCAN achieves superior performance with an average accuracy of 45.68% and 58.91% for 4-class and 5-class LOOCV classification, respectively, which confirms that the adversarial mechanism improves the generalization ability across subjects related to stress classification tasks. EA was applied and the improved generalization ability of EA-SDCAN across subjects was also validated via LOOCV, with the accuracies of four and five stages being 60.52% and

48.17%, respectively. These findings can potentially contribute to the development of more accurate and robust EEG-based stress recognition in real-life applications.

Appendix

The comparison between the SDCAN model and EA-SDCAN model by applying the LOOCV manner is shown in Table VIII. The LOOCV classification performance of the SDCAN, EA-SDCAN, and benchmarking models on each subject are shown in Tables IX.

References

[1] H. Selye, "The stress syndrome," *Amer. J. Nursing*, vol. 65, no. 3, pp. 97–99, Mar. 1965.

[2] N. Sharma and T. Gedeon, "Objective measures, sensors and computational techniques for stress recognition and classification: A survey," *Comput. Methods Programs Biomed.*, vol. 108, no. 3, pp. 1287–1301, Dec. 2012.

[3] C. Espinosa-Garcia, I. Sayeed, and S. Yousuf, "Stress primes microglial polarization after global ischemia: Therapeutic potential of progesterone," *Brain, Behav., Immunity*, vol. 66, pp. 177–192, Nov. 2017.

[4] S. S. Dickerson and M. E. Kemeny, "Acute stressors and cortisol responses: A theoretical integration and synthesis of laboratory research," *Psychol. Bull.*, vol. 130, no. 3, pp. 355–391, May 2004.

[5] J. Hinterdobler *et al.*, "Acute mental stress drives vascular inflammation and promotes plaque destabilization in mouse atherosclerosis," *Eur. Heart J.*, vol. 42, no. 39, pp. 4077–4088, Oct. 2021.

[6] D. H. Hellhammer, S. Wüst, and B. M. Kudielka, "Salivary cortisol as a biomarker in stress research," *Psychoneuroendocrinology*, vol. 34, no. 2, pp. 163–171, Feb. 2009.

[7] M. Groschl, M. Rauh, and H. G. Dorr, "Circadian rhythm of salivary cortisol, 17α-hydroxyprogesterone, and progesterone in healthy children," *Clin. Chem.*, vol. 49, no. 10, pp. 1688–1691, Oct. 2000.

[8] D. S. Dunn, "Stress measurement: Interdisciplinary and state of the art," *Contemp. Psychol., J. Rev.*, vol. 42, no. 1, pp. 56–57, Jan. 1997.

[9] T. K. Liu, Y. P. Chen, Z. Y. Hou, C. C. Wang, and J. H. Chou, "Noninvasive evaluation of mental stress using by a refined rough set technique based on biomedical signals," *Artif. Intell. Med.*, vol. 61, no. 2, pp. 97–103, Jun. 2014.

[10] A. Vyas, R. Mitra, B. S. Shankaranarayana Rao, and S. Chattarji, "Chronic stress induces contrasting patterns of dendritic remodeling in hippocampal and amygdaloid neurons," *J. Neurosci.*, vol. 22, no. 15, pp. 6810–6818, Aug. 2002.

[11] W. S. Liew, M. Seera, C. K. Loo, E. Lim, and N. Kubota, "Classifying stress from heart rate variability using salivary biomarkers as reference," *IEEE Trans. Neural Netw. Learn. Syst.*, vol. 27, no. 10, pp. 2035–2046, Oct. 2016.

[12] C. M. Vander Weele, C. Saenz, J. Yao, S. S. Correia, and K. A. Goosens, "Restoration of hippocampal growth hormone reverses stress-induced hippocampal impairment," *Frontiers Behav. Neurosci.*, vol. 7, p. 66, Jun. 2013.

[13] S. Salim, "Oxidative stress and the central nervous system," *J. Pharmacol. Exp. Therapeutics*, vol. 360, no. 1, pp. 201–205, Jan. 2017.

[14] V. Engert *et al.*, "Investigation into the cross-correlation of salivary cortisol and alpha-amylase responses to psychological stress," *Psychoneuroendocrinology*, vol. 36, no. 9, pp. 1294–1302, Oct. 2011.

[15] H. Alkaf, A. Khandoker, H. Jelinek, and K. Khalaf, "NeuroSky mindwave mobile headset 2 as an intervention for reduction of stress and anxiety measured with pulse rate variability," in *Proc. Comput. Cardiol. Conf. (CinC)*, Rimini, Italy, Dec. 2020, pp. 1–4.

[16] D. Ivaskevych, T. Sergii, and O. Ivaskevych, "MUSE headband design and its impact on the quality of EEG Recording," *Psychophysiology*, vol. 57, p. S68, Oct. 2020.

[17] B. Hjorth, "EEG analysis based on time domain properties," *Electroencephalogr. Clin. Neurophysiol.*, vol. 29, no. 3, pp. 306–310, 1970.

[18] N. H. A. Hamid, N. Sulaiman, S. A. M. Aris, Z. H. Murat, and M. N. Taib, "Evaluation of human stress using EEG power spectrum," in *Proc. 6th Int. Colloq. Signal Process. Appl.*, Malacca, Malaysia, May 2010, pp. 1–4.

[19] A. Arsalan, M. Majid, A. R. Butt, and S. M. Anwar, "Classification of perceived mental stress using a commercially available EEG headband," *IEEE J. Biomed. Health Informat.*, vol. 23, no. 6, pp. 2257–2264, Nov. 2019.

[20] B.-G. Lee and W.-Y. Chung, "Wearable glove-type driver stress detection using a motion sensor," *IEEE Trans. Intell. Transp. Syst.*, vol. 18, no. 7, pp. 1835–1844, Jul. 2017.

[21] S. Pourmohammadi and A. Maleki, "Stress detection using ECG and EMG signals: A comprehensive study," *Comput. Methods Programs Biomed.*, vol. 193, Sep. 2020, Art. no. 105482.

[22] O. M. Mozos *et al.*, "Stress detection using wearable physiological and sociometric sensors," *Int. J. Neural Syst.*, vol. 27, no. 2, Mar. 2017, Art. no. 1650041.

[23] L. Han, Q. Zhang, X. Chen, Q. Zhan, T. Yang, and Z. Zhao, "Detecting work-related stress with a wearable device," *Comput. Ind.*, vol. 90, pp. 42–49, Sep. 2017.

[24] Q. Xu, T. L. Nwe, and C. Guan, "Cluster-based analysis for personalized stress evaluation using physiological signals," *IEEE J. Biomed. Health Inform.*, vol. 19, no. 1, pp. 275–281, Jan. 2015.

[25] S. Betti *et al.*, "Evaluation of an integrated system of wearable physiological sensors for stress monitoring in working environments by using biological markers," *IEEE Trans. Biomed. Eng.*, vol. 65, no. 8, pp. 1748–1758, Aug. 2018.

[26] A. Khorram, M. Khalooei, and M. Rezghi, "End-to-end CNN+LSTM deep learning approach for bearing fault diagnosis," *Appl. Intell.*, vol. 51, no. 2, pp. 736–751, Aug. 2021.

[27] S. F. Naqvi *et al.*, "Real-time stress assessment using sliding window based convolutional neural network," *Sensors*, vol. 20, no. 16, p. 4400, Aug. 2020.

[28] M. A. Almogbel, A. H. Dang, and W. Kameyama, "Cognitive workload detection from raw EEG-signals of vehicle driver using deep learning," in *Proc. 21st Int. Conf. Adv. Commun. Technol. (ICACT)*, PyeongChang, South Korea, Feb. 2019, pp. 1167–1172.

[29] Y. Sun, F. P.-W. Lo, and B. Lo, "EEG-based user identification system using 1D-convolutional long short-term memory neural networks," *Expert Syst. Appl.*, vol. 125, pp. 259–267, Jul. 2019.

[30] I. J. Goodfellow *et al.*, "Generative adversarial networks," in *Proc. Neural Inf. Process. Syst.*, Montreal, QC, Canada, 2014, pp. 2672–2680.

[31] O. Ozdenizci, Y. Wang, T. Koike-Akino, and D. Erdogmus, "Learning invariant representations from EEG via adversarial inference," *IEEE Access*, vol. 8, pp. 27074–27085, 2020.

[32] S. Hwang, M. Ki, K. Hong, and H. Byun, "Subject-independent EEG-based emotion recognition using adversarial learning," in *Proc. 8th Int. Winter Conf. Brain-Comput. Interface (BCI)*, Gangwon, South Korea, Feb. 2020, pp. 99–102.

[33] S. Stober, A. Sternin, and A. M. Owen, "Deep feature learning for EEG recordings," *Comput. Sci.*, vol. 165, pp. 23–31, Jun. 2015.

[34] C. Kirschbaum, "The 'trier social stress test'–A tool for investigating psychobiological stress responses in a laboratory setting," *Neuropsychobiology*, vol. 28, no. 2, pp. 76–81, Jan. 1993.

[35] L. Pbert, L. A. Doerfler, and D. DeCosimo, "An evaluation of the perceived stress scale in two clinical populations," *J. Psychopathol. Behav. Assessment*, vol. 14, no. 4, pp. 363–375, Dec. 1992.

[36] P. Skapinakis, "Spielberger state-trait anxiety inventory," in *Encyclopedia of Quality of Life and Well-Being Research*. Dordrecht, The Netherlands: Springer, 2014, pp. 6261–6264.

[37] W. W. K. Zung, "A self-rating depression scale," *Arch. Gen. Psychiatry*, vol. 12, no. 1, pp. 63–70, Jan. 1965.

[38] A. Delorme and S. Makeig, "EEGLAB: An open source toolbox for analysis of single-trial EEG dynamics including independent component analysis," *J. Neurosci. Methods*, vol. 134, no. 1, pp. 9–21, Mar. 2004.

[39] G. I. T. Salimans and B. W. Zarem, "Improved techniques for training GANs," in *Proc. Adv. Neural Inf. Process. Syst.*, Barcelona Spain, 2016, pp. 2234–2242.

[40] V. J. Lawhern *et al.*, "EEGNet: A compact convolutional neural network for EEG-based brain–computer interfaces," *J. Neural Eng.*, vol. 15, no. 5, 2018, Art. no. 056013.

[41] R. T. Schirrmeister *et al.*, "Deep learning with convolutional neural networks for EEG decoding and visualization," *Hum. Brain Mapping*, vol. 38, no. 11, pp. 5391–5420, Nov. 2017.

[42] H. S. Kim, D. Yoon, H. S. Shin, and C. H. Park, "Predicting the EEG level of a driver based on driving information," *IEEE Trans. Intell. Transp. Syst.*, vol. 20, no. 4, pp. 1215–1225, Apr. 2019.

[43] C. K. A. Lim and W. C. Chia, "Analysis of single-electrode EEG rhythms using MATLAB to elicit correlation with cognitive stress," *Int. J. Comput. Theory Eng.*, vol. 7, no. 2, p. 419, Apr. 2015.

[44] H. He and D. Wu, "Transfer learning for brain–computer interfaces: A Euclidean space data alignment approach," *IEEE Trans. Biomed. Eng.*, vol. 67, no. 2, pp. 399–410, Feb. 2020.

[45] D. Hardoon, S. Szedmak, and J. Shawe-Taylor, “Canonical correlation analysis: An overview with application to learning methods,” *Neural Comput.*, vol. 16, no. 12, pp. 2639–2664, Dec. 2004.
[46] A. Kamrud, B. Borghetti, and C. S. Kabban, “The effects of individual differences, non-stationarity, and the importance of data partitioning decisions for training and testing of EEG cross-participant models,” *Sensors*, vol. 21, no. 9, p. 3225, May 2021.
[47] L. Gonzalez-Carabarin, E. A. Castellanos-Alvarado, P. Castro-Garcia, and M. A. Garcia-Ramirez, “Machine learning for personalised stress detection: Inter-individual variability of EEG-ECG markers for acute-stress response,” *Comput. Methods Programs Biomed.*, vol. 209, Sep. 2021, Art. no. 106314.
[48] V. Vanitha and P. Krishnan, “Real time stress detection system based on EEG signals,” *Biomed. Res.-India*, vol. 27, pp. S271–S275, Jan. 2016.
[49] H. He and D. Wu, “Different set domain adaptation for brain-computer interfaces: A label alignment approach,” *IEEE Trans. Neural Syst. Rehabil. Eng.*, vol. 28, no. 5, pp. 1091–1108, May 2020.
[50] R. Miller *et al.*, “How to disentangle psychobiological stress reactivity and recovery: A for comparison of model-based and non-compartmental analyses of cortisol concentrations,” *Psychoneuroendocrinology*, vol. 90, pp. 194–210, Apr. 2018.
[51] F. Spiga *et al.*, “HPA axis-rhythms,” *Compr Physiol.*, vol. 4, no. 3, pp. 1273–1298, Jul. 2014.
[52] N. F. Narvaez Linares, V. Charron, A. J. Ouimet, P. R. Labelle, and H. Plamondon, “A systematic review of the trier social stress test methodology: Issues in promoting study comparison and replicable research,” *Neurobiol. Stress*, vol. 13, Nov. 2020, Art. no. 100235.
[53] A. P. Allen, P. J. Kennedy, J. F. Cryan, T. G. Dinan, and G. Clarke, “Biological and psychological markers of stress in humans: Focus on the trier social stress test,” *Neurosci. Biobehav. Rev.*, vol. 38, pp. 94–124, Jan. 2014.
[54] Y. Xin, J. Wu, Z. Yao, Q. Guan, A. Aleman, and Y. Luo, “The relationship between personality and the response to acute psychological stress,” *Sci. Rep.*, vol. 7, no. 1, p. 16906, Dec. 2017.
[55] I. Labuschagne, C. Grace, P. Rendell, G. Terrett, and M. Heinrichs, “An introductory guide to conducting the trier social stress test,” *Neurosci. Biobehav. Rev.*, vol. 107, pp. 686–695, Dec. 2019.
[56] A. I. Turner *et al.*, “Psychological stress reactivity and future health and disease outcomes: A systematic review of prospective evidence,” *Psychoneuroendocrinology*, vol. 114, Apr. 2020, Art. no. 104599.
[57] A. L. Shilton, R. Laycock, and S. G. Crewther, “The Maastricht acute stress test (MAST): Physiological and subjective responses in anticipation, and post-stress,” *Frontiers Psychol.*, vol. 8, pp. 567–577, Apr. 2017.
[58] S. A. Unde and R. Shriram, “PSD based coherence analysis of EEG signals for stroop task,” *Int. J. Comput. Appl.*, vol. 95, no. 16, pp. 1–5, Jun. 2014.
[59] L. Schwabe and H. Schächinger, “Ten years of research with the socially evaluated cold pressor test: Data from the past and guidelines for the future,” *Psychoneuroendocrinology*, vol. 92, pp. 155–161, Jun. 2018.